Convex Optimization In Identification Of Stable Non-Linear State Space Models

Mark M. Tobenkin[1] Ian R. Manchester[1] Jennifer Wang[2] Alexandre Megretski[3] Russ Tedrake[1]

1: Computer Science and Artificial Intelligence Laboratory, Massachusetts Inst. of Tech.
2: Department of Brain and Cognitive Sciences, Massachusetts Inst. of Tech.
3: Laboratory for Information and Decision Systems, Massachusetts Inst. of Tech.
{mmt, irm, jenwang, ameg, russt}@mit.edu

***Abstract*— A new framework for nonlinear system identification is presented in terms of optimal fitting of stable nonlinear state space equations to input/output/state data, with a performance objective defined as a measure of robustness of the simulation error with respect to equation errors. Basic definitions and analytical results are presented. The utility of the method is illustrated on a simple simulation example as well as experimental recordings from a live neuron.**

I. Introduction

Converting numerical data, originating from either physical measurements or computer simulations, to compact mathematical models is a common challenge in engineering. The case of *static system identification*, where models $y = h(u)$ defined by "simple" functions $h(\cdot)$ are fitted to data records of u and y, is a major topic of research in *statistics* and *machine learning*. This paper is focused on a subset of *dynamic system identification* tasks, where state space models of the form

$$x(t+1) = f(x(t), u(t)), \quad (1)$$
$$y(t) = g(x(t), u(t)), \quad (2)$$

where f and g are "simple" functions, are extracted from data records of $\tilde{x}, \tilde{y}$, and $\tilde{u}$. We will also consider continuous time models of the form

$$\dot{x}(t) = f(x(t), u(t)), \quad (3)$$

with (2). If the data come from simulations of a complex model rather than experiments then this task is referred to as *model reduction*.

There are two common and straightforward approaches to this problem: In *equation-error minimization* (see, e.g., [1], [2]) a model is sought which minimizes a cost function of the following form: $\sum_t |\tilde{x}(t+1) - f(\tilde{x}(t), \tilde{u}(t))|^2$, or similar, over the unknown parameters of $f(\cdot)$. A similar optimization can be set up for $g(\cdot)$. This is typically very cheap computationally, often reducing to basic least squares. However, if there is no incremental stability requirement then small equation errors do not imply small simulation errors over extended time intervals. For large scale and nonlinear problems it is not unusual to find unstable models by this method, particularly if the true system is not in the model class being searched over.

This was supported by National Science Foundation Grant No. 0835947.

In *Simulation-error minimization* (see, e.g., [3]) one sets up a nonlinear programming problem to find $\min_\eta \sum_t |\tilde{y}(t) - y_\eta(t)|^2$ where y_η is the output of the simulation of the model system with a particular set of parameters η which define $f(\cdot)$ and $g(\cdot)$. If successful, this can give a more robust fit than equation error. However, the relationship between the unknown parameters η and the long-term simulation $y_\eta(t)$ is highly nonlinear and the optimization nonconvex. For black-box models with a large number of parameters, this optimization can be very difficult.

The method proposed in this paper can be considered a middle-ground between these two extremes: we formulate a convex optimization problem to minimize an *upper bound* on the true simulation error while guaranteeing the stability and well-posedness of the identified model. Furthermore, we show that that in some simple cases the upper bound is tight.

Other recent efforts on identification of guaranteed stable models include LMI conditions for linear systems [4], convex relaxations for linear [5] and Wiener-Hammerstein systems [6], as well as passivity-like conditions for linear [7] and nonlinear models [8].

We are freely providing a MATLAB implementation of the proposed technique as part of SPOT [9].

II. Problem Setup

A. State Space Models

We examine discrete time (DT) state space models of the form

$$e(x(t+1)) = f(x(t), u(t)), \quad (4)$$
$$y(t) = g(x(t), u(t)), \quad (5)$$

where $e : \mathbb{R}^n \mapsto \mathbb{R}^n$, $f : \mathbb{R}^n \times \mathbb{R}^m \mapsto \mathbb{R}^n$, and $g : \mathbb{R}^n \times \mathbb{R}^m \mapsto \mathbb{R}^k$ are continuously differentiable functions such that the equation $e(z) = w$ has a unique solution $z \in \mathbb{R}^n$ for every $w \in \mathbb{R}^n$.

B. Stability

We consider the DT model (4),(5) *stable* if the difference $\{y_1(t) - y_0(t)\}_{t=1}^\infty$ is square summable for every two solutions $(u, x, y) = (u_1, x_1, y_1)$ and $(u, x, y) = (u_0, x_0, y_0)$ of

(4),(5) with the same input $u_1 = u_0 = u$. This definition can be qualified as that of *global incremental output ℓ_2-stability*.

C. Data

In applications, we expect to have input/state/output information available in the form of *sampled data* $\tilde{\mathcal{Z}} = \{\tilde{z}(t_i)\}_{i=1}^N$, where $\tilde{z}(t_i) = (\tilde{v}(t_i), \tilde{x}(t_i), \tilde{u}(t_i), \tilde{y}(t_i))$. Here $\tilde{x}, \tilde{u}, \tilde{y}$ represent approximated samples of state, input, and output respectively, and $\tilde{v}$ approximates the "next" state. Section VI-A will discuss approaches for approximating the state of the system from input-output data.

For the purpose of theoretical analysis, we will assume that the input/state/output information is available in the form of *signal data* where $\tilde{v}$, $\tilde{x}$, $\tilde{u}$, and $\tilde{y}$ are *signals*, i.e. functions

$$\tilde{x}, \tilde{v} : \mathcal{T} \mapsto \mathbb{R}^n, \ \tilde{u} : \mathcal{T} \mapsto \mathbb{R}^m, \ \tilde{y} : \mathcal{T} \mapsto \mathbb{R}^k \tag{6}$$

such that

$$\mathcal{T} = \{1, \dots, N\}, \quad \tilde{v}(t-1) = \tilde{x}(t) \ \forall \ t \in \{2, \dots, N\}. \tag{7}$$

D. Simulation Error

Given DT *signal data* $\tilde{\mathcal{Z}}$ and functions e, f, g, the *simulation error* associated with a model matching (4),(5) is defined as

$$\bar{\mathcal{E}} = \sum_{t=1}^{N} |\tilde{y}(t) - y(t)|^2, \tag{8}$$

where $y(t)$ is defined by (4),(5) with $u(t) \equiv \tilde{u}(t)$ and $x(1) = \tilde{x}(1)$.

E. Linearized Simulation Error

A simplified version of the simulation error measure $\bar{\mathcal{E}}$ is the *linearized simulation error* $\bar{\mathcal{E}}^0$ defined in the following way. Consider a "perturbed" version of the system equations

$$e(x_\theta(t+1)) = f(x_\theta(t), u(t)) - f_0(t), \tag{9}$$
$$y_\theta(t) = g(x_\theta(t), u(t)) - g_0(t). \tag{10}$$

Here $\theta \in [0, 1]$, $f_0(t) = (1-\theta)\epsilon_x(\tilde{z}(t))$, and $g_0(t) = (1-\theta)\epsilon_y(\tilde{z}(t))$, where ϵ_x and ϵ_y are the *equation errors* are defined by:

$$\epsilon_x(\tilde{z}) = f(\tilde{x}, \tilde{u}) - e(\tilde{v}), \tag{11}$$
$$\epsilon_y(\tilde{z}) = g(\tilde{x}, \tilde{u}) - \tilde{y}. \tag{12}$$

We examine the solution (x_θ, y_θ) of (9),(10) with $x_\theta(1) = \tilde{x}(1)$, $u(t) \equiv \tilde{u}(t)$.

By construction, $y_\theta = y$ for $\theta = 1$, and $y_\theta = \tilde{y}$ for $\theta = 0$. We define

$$\bar{\mathcal{E}}^0(\tilde{z}(t)) = \lim_{\theta \to 0} \frac{1}{\theta^2} \sum_{t=1}^{N} |\tilde{y}(t) - y_\theta(t)|^2 \tag{13}$$

to quantify local sensitivity of model equations with respect to equation errors.

Using standard linearization analysis, it is easy to produce alternative expressions for $\bar{\mathcal{E}}^0$:

$$\bar{\mathcal{E}}^0 = \sum_{t=1}^{N} |G(\tilde{x}(t), \tilde{u}(t))\tilde{\Delta}(t) + \epsilon_y(\tilde{z}(t))|^2, \tag{14}$$

where $\tilde{\Delta}(\cdot)$ is defined by

$$E(\tilde{x}(t+1))\tilde{\Delta}(t+1) = F(\tilde{x}(t), \tilde{u}(t))\tilde{\Delta}(t) + \epsilon_x(\tilde{z}(t)), \tag{15}$$

with initial condition $\tilde{\Delta}(1) = 0$, and $E = E(x), F = F(x, u)$ and $G = G(x, u)$ defined to be the Jacobians (with respect to x) of e, f and g respectively.

F. Optimization Setup

Within the framework of this paper, we consider efficient global minimization of the simulation error $\bar{\mathcal{E}}$ (over all model functions e, f, g, defining a stable system) as an ultimate (if perhaps unattainable) goal. We proceed by defining upper bounds for $\bar{\mathcal{E}}$ and $\bar{\mathcal{E}}^0$ which can be minimized efficiently by means of convex optimization (semidefinite programming). We will also prove some theoretical statements certifying quality of these upper bounds.

III. Robust Identification Error

The dependence of the simulation error ($\bar{\mathcal{E}}$ or $\bar{\mathcal{E}}^0$) on the coefficients of system equations (4),(5) is complicated enough to make it a challenging object for efficient global minimization, especially under the stability constraint. The objective of this section is to introduce several versions of *robust identification error* (RIE) - a sample-wise measure of simulation error, motivated by the idea of using storage functions and dissipation inequalities to generate useful upper bounds of $\bar{\mathcal{E}}$ and $\bar{\mathcal{E}}^0$.

A. Global RIE

The global RIE measure for a DT model (4),(5) is a function of the coefficients of (4),(5), a single data sample

$$\tilde{z} = (\tilde{v}, \tilde{x}, \tilde{u}, \tilde{y}) \in \mathbb{R}^n \times \mathbb{R}^n \times \mathbb{R}^m \times \mathbb{R}^k, \tag{16}$$

and an auxiliary parameter $Q = Q' > 0$, a positive definite symmetric n-by-n matrix (for convenience, we only indicate the dependence on $\tilde{z}$ and Q):

$$\mathcal{E}_Q(\tilde{z}) = \sup_{\Delta \in \mathbb{R}^n} \left\{ |f(\tilde{x} + \Delta, \tilde{u}) - e(\tilde{v})|_Q^2 - |\delta_e|_Q^2 + |\delta_y|^2 \right\}. \tag{17}$$

where $|a|_Q^2$ is a shortcut for $a'Qa$, and

$$\delta_e = e(\tilde{x} + \Delta) - e(\tilde{x}), \quad \delta_y = g(\tilde{x} + \Delta, \tilde{u}) - \tilde{y}. \tag{18}$$

The following statement explains the utility of the RIE measure in generating upper bounds of simulation error.

Theorem 1: The inequality

$$\bar{\mathcal{E}} \le \sum_{t=1}^{N} \mathcal{E}_Q(\tilde{z}(t)), \tag{19}$$

holds for every $Q = Q' > 0$ and signal data (6),(7).

B. Local RIE

The local RIE for a DT model (4),(5) is defined by:

$$\mathcal{E}^0_Q(\tilde{z}) = \sup_{\Delta\in\mathbb{R}^n} \left\{ |F\Delta + \epsilon_x|^2_Q - |E\Delta|^2_Q + |G\Delta + \epsilon_y|^2 \right\}, \tag{20}$$

and provides an upper bound for the linearized simulation error $\bar{\mathcal{E}}^0$ according to the following statement.

Theorem 2: The inequality

$$\bar{\mathcal{E}}^0 \le \sum_{t=1}^{N} \mathcal{E}^0_Q(\tilde{z}(t)), \tag{21}$$

holds for every $Q = Q' > 0$ and signal data (6),(7).

Note that the supremum in (20) is finite if and only if the matrix $R_{dt} = F'QF - E'QE + G'G$ is negative semidefinite. In applications, *strict* negative definiteness of the matrix R_{dt} is enforced, to be referred to as *robustness* of the corresponding supremum.

C. RIE and Stability

The following theorem shows that global finiteness of the local RIE implies global stability of the model (4),(5).

Theorem 3: Let continuously differentiable functions f, g, e and matrix $Q = Q' > 0$ be such that e has a smooth inverse e^- (i.e. $e^-(e(x)) = e(e^-(x)) = x$ for all $x \in \mathbb{R}^n$), and $\mathcal{E}^0_Q(e^-(f(x,u)), x, u, g(x,u))$ is finite for every $x \in \mathbb{R}^n$, $u \in \mathbb{R}^m$. Then system (4),(5) is globally incrementally output ℓ_2-stable.

IV. A Convex Upper Bound for Optimization

The results of the previous section suggest minimization (with respect to e, f, g, Q) of the sum of RIE over the available data points as an approach to system identification. However, in general, the RIE functions are *not* convex with respect to e, f, g and Q. In this section, we use the inequality

$$-a'Qa \le \Delta' Q^{-1}\Delta - 2\Delta' a, \tag{22}$$

which, due to the identity

$$\Delta' Q^{-1}\Delta - 2\Delta' a + a'Qa = |a - Q^{-1}\Delta|^2_Q,$$

is valid for all $a, \Delta \in \mathbb{R}^n$ and a real symmetric n-by-n matrix Q such that $Q = Q' > 0$, to derive a family of upper bounds for the RIE functions. The upper bounds will be jointly convex with respect to e, f, g, and $P = Q^{-1} > 0$.

A. Upper Bounds for Global RIE in Discrete Time

Given a symmetric positive definite n-by-n matrix Q and functions $e:\ \mathbb{R}^n \mapsto \mathbb{R}^n$ and $f:\ \mathbb{R}^n \times \mathbb{R}^m \mapsto \mathbb{R}^n$, let

$$\delta_v \quad = \quad f(\tilde{x} + \Delta, \tilde{u}) - e(\tilde{v}).$$

Applying (22) with $a = \delta_e$ to the $-|\delta_e|^2_Q$ term in the definition of $\mathcal{E}_Q(\tilde{z})$ yields $\mathcal{E}_Q(\tilde{z}) \le \hat{\mathcal{E}}_Q(\tilde{z})$ where

$$\hat{\mathcal{E}}_Q(\tilde{z}) = \sup_{\Delta\in\mathbb{R}^n} \left\{ |\delta_v|^2_Q + |\Delta|^2_P - 2\Delta'\delta_e + |\delta_y|^2 \right\}, \tag{23}$$

and $P = Q^{-1}$. The function $\hat{\mathcal{E}}_Q(\tilde{z})$ serves as an upper bound for $\mathcal{E}_Q(\tilde{z})$ that is again jointly convex with respect to e, f, g, and $P = Q^{-1} > 0$.

B. Upper Bounds for Local RIE in Discrete Time

Given a symmetric positive definite n-by-n matrix Q and functions $e:\ \mathbb{R}^n \mapsto \mathbb{R}^n$, $f:\ \mathbb{R}^n \times \mathbb{R}^m \mapsto \mathbb{R}^n$ let

$$\Delta_e = E(\tilde{x})\Delta,\ \Delta_v = F(\tilde{x}, \tilde{u})\Delta + \epsilon_x,\ \Delta_y = G(\tilde{x}, \tilde{u})\Delta + \epsilon_y.$$

Applying (22) with $a = \Delta_e$, to the $-|\Delta_e|^2_Q$ term in the definition of $\mathcal{E}_Q(\tilde{z})$ yields $\mathcal{E}_Q(\tilde{z}) \le \hat{\mathcal{E}}^0_Q(\tilde{z})$ where

$$\hat{\mathcal{E}}^0_Q(z) = \sup_{\Delta\in\mathbb{R}^n} \left\{ |\Delta_v|^2_Q + |\Delta|^2_P - 2\Delta'\Delta_e + |\Delta_y|^2 \right\}, \tag{24}$$

with $P = Q^{-1}$. The function $\hat{\mathcal{E}}^0_Q(\tilde{z})$ serves as an upper bound for $\mathcal{E}^0_Q(\tilde{z})$ that is jointly convex with respect to e, f, g, and $P = Q^{-1} > 0$.

C. Well-Posedness of State Dynamics

This well-posedness of state dynamics equation (4) is guaranteed when the function $e:\ \mathbb{R}^n \mapsto \mathbb{R}^n$ is a bijection. The well-posedness of (4) is implied by robustness of the supremum in the definition (24) of the upper bound $\hat{\mathcal{E}}^0_Q$ of the local RIE $\mathcal{E}^0_Q$, i.e. by strict negative definiteness of the matrix: $\hat{R}_{dt} = F'QF + P - E' - E + G'G$. Note that this is not guaranteed by the robustness of (20).

Theorem 4: Let $e:\ \mathbb{R}^n \mapsto \mathbb{R}^n$ be a continuously differentiable function with a uniformly bounded Jacobian $E(x)$, satisfying:

$$E(x) + E(x)' \ge 2r_0 I, \quad \forall x \in \mathbb{R}^n \tag{25}$$

for some fixed $r_0 > 0$. Then e is a bijection.

When $e(x)$ is nonlinear one can solve for $\hat{x}$ such that $|\hat{x} - x_0| < \epsilon$ (with $e(x_0) = z$) via the ellipsoid method, or related techniques. Given a guess $\hat{x}$, we know the true solution lies in a sphere: $|e(\hat{x}) - z| \ge r_0|\hat{x} - x_0|$. Further, we have a cutting plane oracle: $(\hat{x} - x_0)'(e(\hat{x}) - z) \ge 0$.

D. Coverage of Stable Linear Systems

Since we have produced an upper bound for the simulation error both through the introduction of $\mathcal{E}_Q(\tilde{z})$ and $\hat{\mathcal{E}}_Q(\tilde{z})$, it is desirable to check whether a basic class of systems will be recovered exactly.

Consider a linear system

$$x(t+1) = Ax(t) + Bu(t),\ y(t) = Cx(t) + Du(t)$$

where $x \in \mathbb{R}^n$ and $u \in \mathbb{R}^m$. Define the "data matrices" from an experiment of length N to be $X := [\tilde{x}(t_1), \ldots, \tilde{x}(t_N)]$, $U := [\tilde{u}(t_1), \ldots, \tilde{u}(t_N)]$. Suppose we have fit a linear model

$$Ex(t+1) = Fx(t) + Lu(t),\ y(t) = Gx(t) + Hu(t).$$

We consider a linear system to have been recovered exactly by the model if $G = C, D = H, EB = L$, and $EA = F$.

Theorem 5: For data generated from a stable DT linear system with zero noise, if the data matrix $[X', U']'$ is of rank at least $n + m$, then the linear system is recovered exactly and $\mathcal{E}_Q(\tilde{z}) = \hat{\mathcal{E}}_Q(\tilde{z}) = 0$.

Note that by construction for the case of a linear model $\mathcal{E}_Q = \mathcal{E}^0_Q$. In order to prove this theorem, we will use the following lemma:

Lemma 1: For any Schur matrix A there exists E, F and $Q > 0$ such that $EA = F$ satisfying $M = M' < 0$ where

$$M := F'QF + Q^{-1} - E' - E + G'G. \tag{26}$$

Proof of Theorem 5. Using the choice of E, F, Q in Lemma 1, since the data is noise free and $EA = F$ we have $\epsilon_x = \epsilon_y = 0$. As a result, it follows from Lemma 1 that $\hat{\mathcal{E}}_Q(\tilde{z})$ is the supremum of a homogeneous negative-definite quadratic form in Δ, hence has a value of zero. Similarly, with zero noise (20) is the supremum of a homogeneous quadratic form in Δ and since $\mathcal{E}_Q(\tilde{z}) \leq \hat{\mathcal{E}}_Q(\tilde{z}) = 0$ we have $\mathcal{E}_Q(\tilde{z}) = 0$. The rank condition on the data matrices ensures that if robust equation error is zero, then the true system is recovered. ∎

V. Continuous Time Results

Our continuous time results are presented in full in [10]. Here we simply provide definitions.

For continuous time (CT) models, (4) is replaced by

$$E(x(t))\dot{x}(t) \quad = \quad f(x(t), u(t)), \tag{27}$$

where $E(x)$ is the Jacobian of $e(\cdot)$ at x. Naturally, $E(x)$ is required to be non-singular for all x. We consider the model (5),(27) is *stable* if the difference $y_1 - y_0$ is square integrable for every two solutions $(u, x, y) = (u_1, x_1, y_1)$ and $(u, x, y) = (u_0, x_0, y_0)$ of (5),(27) with the same input $u_1 = u_0 = u$. We assume we have access to samples input/state/output data $(\tilde{u}, \tilde{x}, \tilde{y})$ as well as $\tilde{v} = \frac{d}{dt}\tilde{x}$.

The simulation error is defined as:

$$\bar{\mathcal{E}} = \int_0^T |\tilde{y}(t) - y(t)|^2 dt, \tag{28}$$

where y is defined by (5),(27) with $u(t) \equiv \tilde{u}(t)$ and $x(0) = \tilde{x}(0)$. The equation error (11) is replaced by:

$$\epsilon_x(\tilde{z}) = f(\tilde{x}, \tilde{u}) - E(\tilde{x})\tilde{v} \tag{29}$$

Via a linearized analysis similar to Section II-E we have:

$$\bar{\mathcal{E}}^0 = \int_0^T |G(\tilde{x}(t), \tilde{u}(t))\tilde{\Delta}(t) + \epsilon_y(\tilde{z}(t))|^2 dt, \tag{30}$$

where $\tilde{\Delta}(\cdot)$ is defined by an initial condition $\tilde{\Delta}(0) = 0$ and:

$$\frac{d}{dt}[E(\tilde{x}(t))\tilde{\Delta}(t)] = F(\tilde{x}(t), \tilde{u}(t))\tilde{\Delta}(t) + \epsilon_x(\tilde{z}(t)). \tag{31}$$

The *global RIE* is given by:

$$\mathcal{E}_Q(\tilde{z}) = \sup_{\Delta \in \mathbb{R}^n} \left\{ 2\delta_e' Q[f(\tilde{x} + \Delta, \tilde{u}) - E(\tilde{x})\tilde{v}] + |\delta_y|^2 \right\}, \tag{32}$$

and the *local RIE* is given by:

$$\mathcal{E}_Q^0(z) = \sup_{\Delta \in \mathbb{R}^n} \left\{ 2(E\Delta)'Q(F\Delta + \epsilon_x) + |G\Delta + \epsilon_y|^2 \right\} \tag{33}$$

Similar results to Theorems (1) and (2) are available in [10]. Similarly, global finiteness of the local RIE implies global incremental output $\mathcal{L}_2$-stability.

The upper bound for the global RIE is:

$$\hat{\mathcal{E}}_Q(\tilde{z}) = \sup_{\Delta \in \mathbb{R}^n} \left\{ \frac{|\delta_e^+|_Q^2 + |\Delta|_P^2}{2} - \Delta'\delta_e^- + |\delta_y|^2 \right\}, \tag{34}$$

where $\delta_e^+ = \delta_e + f(\tilde{x} + \Delta, \tilde{u}) - E(\tilde{x})\tilde{v}$ and $\delta_e^- = \delta_e - f(\tilde{x} + \Delta, \tilde{u}) + E(\tilde{x})\tilde{v}$. The upper bound for the local RIE is:

$$\hat{\mathcal{E}}_Q^0(z) = \sup_{\Delta \in \mathbb{R}^n} \left\{ \frac{|\Delta_e^+|_Q^2 + |\Delta|_P^2}{2} - \Delta'\Delta_e^- + |\Delta_y|^2 \right\}, \tag{35}$$

with $\Delta_e^+ = E(\tilde{x})\Delta + F(\tilde{x}, \tilde{u})\Delta + \epsilon_x$ and $\Delta_e^- = E(\tilde{x})\Delta - F(\tilde{x}, \tilde{u})\Delta - \epsilon_x$.

The well-posedness of the dynamics are implied by the invertibility of $E(\cdot)$, or the robustness of the supremum (33). A proof for recovery of linear systems similar to Theorem 5 is available in [10].

VI. Implementation Details

A. Approximating States

The RIE formulation assumes access to approximate state observations, $\tilde{x}(t)$. In most cases of interest, the full state of the system is not directly measurable. In practice, our solutions have been motivated by the assumption that future output can be approximated as a function of recent input-output history and future input. To summarize recent history, we have had success applying linear filter banks, as is common in linear identification (e.g. Laguerre filters [11]).

Even in fairly benign cases one expects the input-output histories to live near a nonlinear submanifold of the space of possible histories. As a result, linear projection based methods may require excessive dimensionality to approximate the state of the system. Connections between nonlinear dimensionality reduction and system identification have recently been explored [12], [13].

For CT identification estimating the rates of the system, $v(t) = \frac{d}{dt}x(t)$, presents an additional challenge. For true system outputs, this can be approached via differentiation filters, or noncausal smoothing before numerical differentiation. Approximating additional states through filter banks allows the rates of these variables to be calculated analytically.

B. Quality of Fit with Semidefinite Programs

For any tuple of data, $\tilde{z}(t_i)$, the upper bound on the local RIE is the supremum of a concave quadratic form in Δ. So long as e, f and g are chosen to be linear in the decision variables, this upper bound can be minimized by introducing an LMI for each data-point using the Schur complement. We introduce a slack variable s_i for each data-point:

$$s_i \geq \hat{\mathcal{E}}_Q^0(\tilde{z}(t_i)), \tag{36}$$

which is a convex constraint and optimize for $\sum_i s_i \to \min$.

Similarly, the upper bound on the global RIE is a function of Δ for fixed $\tilde{z}(t_i)$. If we take e, f and g to be polynomials or rational functions with fixed denominators then the upper bound will be a polynomial or rational function in Δ. As a result, we can minimize this function by introducing a sum-of-squares (SOS) constraint [14]. We again introduce a slack variable s_i:

$$s_i \geq \hat{\mathcal{E}}_Q(\tilde{z}(t_i)), \tag{37}$$

and optimize for $\sum_i s_i \to \min$. This equation will be polynomial in Δ and quadratic in $n+1$ other variables due to

the Schur complement. In most cases, replacing the positivity constraint with a SOS constraint is another convex relaxation.

When fitting a linear (affine) model for (4),(5) or (5),(27) it is interesting to note that $\hat{\mathcal{E}} = \hat{\mathcal{E}}^0$ and further the SDP can be posed to grow only with the dimension of the state, rather than the number of data points. Details are available in [10].

C. Choice of Basis and Stability

Global finiteness of the the upper bound $\hat{\mathcal{E}}_Q^0$ guarantees stability. For a fixed (x, u), boundedness can be verified via an LMI. Taking a polynomial or rational function basis for e, f and g, we can verify this LMI for all (x, u) using a SOS constraint. Global verification of the inequalities places some constraints on the degrees of these polynomials. For example, in DT the degree of $E(x)$ must be able to be twice that of $F(x, u)$ for the inequality to hold globally.

In continuous time, we use the following parametrization to allow for global stability verification:

$$e(x) = \frac{\bar{e}(x)}{q(x)}, \qquad f(x) = \frac{\bar{f}(x,u)}{q(x)p(u)}. \tag{38}$$

Here $q(x) : \mathbb{R}^n \mapsto \mathbb{R}$ is a fixed polynomial of degree $2d_x$ in each x_i such that $q(x) \geq 1$. Similarly $p(u) : \mathbb{R}^m \mapsto \mathbb{R}$ is of degree $2d_u$ in each u_i, and $p(u) \geq 1$. The numerators, $\bar{f}(x, u)$ and $\bar{e}(x)$ are polynomials whose coefficients are decision variables. Both $\bar{e}(x)$ and $\bar{f}(x, u)$ are degree $2d_x + 1$ in each x_i and $\bar{f}$ is of degree $2d_u$ in each u_i.

With these choices of degrees, it is possible for the convex relaxation to be satisfied for all (x, u). The positivity of the expression can be tested via a SOS decomposition. In particular, we choose $q(x)$ and $p(u)$ to be nearly constant over the range of the observed data. For example, we take:

$$q(x) = (1 + \|x\|_2^2)^{d_x} \quad p(u) = (1 + \|u\|_2^2)^{d_u} \tag{39}$$

In general, centering and normalizing the data drastically improves numerical properties of the method. Here, rescaling the data such that it lies in a unit ball around the origin makes this choice of q and p apply more generally.

When global stability is not required, care must be taken to ensure that solutions to the implicit form equations still exist. In continuous time this is guaranteed if $E(x)$ is invertible for all x, and similarly it is guaranteed if $e(x)$ is invertible in discrete time. Both of these constraints can be satisfied by requiring $E(x)+E(x)' \geq 2r_0 I$, which can again be enforced using a SOS constraint.

VII. Examples and Discussion

A. Stability and Noise

In situations with large measurement noise, we have observed that RIE minimization produces models which are more stable (e.g. damped for linear systems) than the system being fit. This is most evident in highly resonant, or nearly marginally stable systems. In these situations, we have had success minimizing equation error while simply requiring the local RIE to be finite at the sample points. Mitigating this effect is a focus of future work.

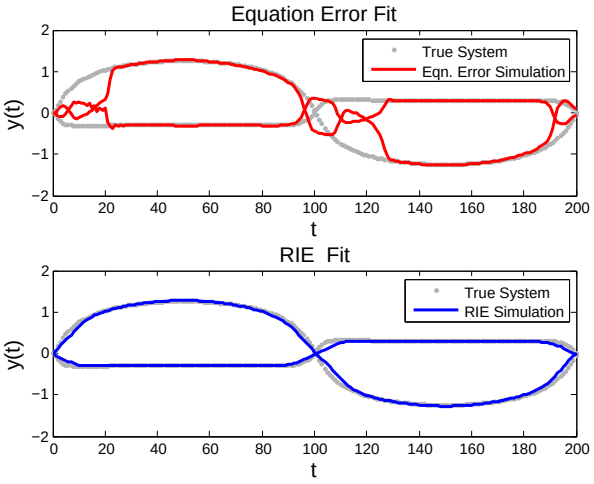

Fig. 1. A comparison of equation error minimization and local RIE minimization on a simulated, second-order, nonlinear discrete time system. The true system response to validation input is compared to an equation error fit (top) and local RIE fit (bottom). The system is not within the model class being searched over.

B. Simulated DT Example

We consider a second-order nonlinear simulated discrete time system:

$$\begin{bmatrix} 2v_1 + v_2^2 v_1 + \frac{1}{3}v_1^5 \\ v_1 + 2v_2 + v_1^2 v_2 + \frac{1}{3}v_2^5 \end{bmatrix} = \begin{bmatrix} 0.4 & -0.9 \\ 0.9 & 0.4 \end{bmatrix} x + \begin{bmatrix} u \\ 0 \end{bmatrix}, \tag{40}$$

where $x = [x_1(t)\, x_2(t)]'$ and $v_i(t) = x_i(t+1)$. For training we excite the system with a chirp: $\tilde{u}(t) = 4\sin(2\pi \frac{10}{500^2} t^2)$ for $t \in \{1, \ldots, 500\}$. We observe $\tilde{y}(t) = \tilde{x}(t) = x(t) + w(t)$, where $w(t)$ is zero mean, Gaussian i.i.d. measurement noise with covariance = $0.0025I$ and independent of $x(t)$.

We fit a model (4),(5) with $g(\cdot, \cdot)$ fixed *a priori* to be $g(x, u) = x$. We choose $e(\cdot)$ to be cubic, and $f(\cdot, \cdot)$ to be a linear combination of u and the monomials up to total degree 7 in the x_i. With these choices the true system is outside the model class. We compare minimizing the local RIE and minimizing equation error. In both cases, we restrict $E + E' > 2I$ ensure the model is well-posed. Figure (1) presents the response of the true system and models for the input $u_{\text{test}}(t) = 4\sin(2\pi \frac{1}{200} t)$ over $t \in \{1, \ldots, 200\}$.

C. Modeling of Post-spike Dynamics in Live Neurons

Our second example is drawn from the task of identifying the response of the membrane potential of a live neuron. Details of the experimental procedure are given in the appendix. In particular, we are interested in identifying the dynamics of the neuron immediately following an action potential.

We excite the neuron with 27 separate multisine input currents. The excitation is applied via a zero-order hold. The response is the sampled membrane potential of the neuron, $\tilde{y}(t)$. Both measurement and control have a sampling rate of 10 kHz. This data set consists of 22 spikes which were separated into equal size training and testing sets.

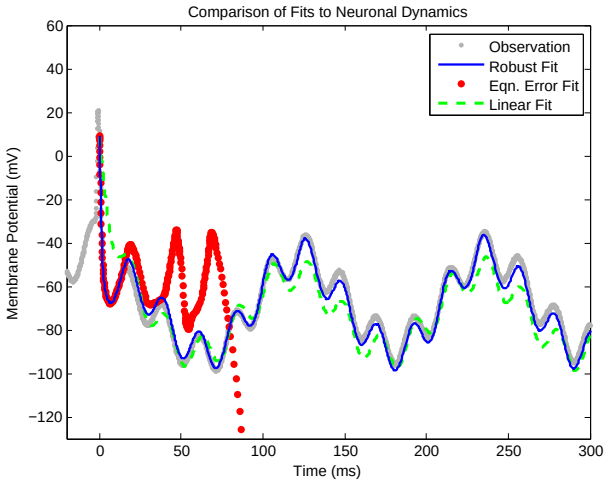

Fig. 2. We compare several fits of the post-spike dynamics of a live neuronal cell on validation data. The "Robust Fit" corresponds to minimizing the local RIE, and is compared to both linear and nonlinear fits minimizing equation error. By $t = 100$, the nonlinear equation error fit has diverged. The linear fit does not capture the steep descent at $t = 0$, nor does it replicate the long term behavior.

To achieve a 3rd order CT fit of the system, we pass the observed output voltage, $\tilde{y}(t)$, through a filter bank determined by the first two Laguerre functions with a pole at 300 radians per second [11]. The original voltage and the output of this filter bank give us $\tilde{x}(t) \in \mathbb{R}^3$. To compute $\tilde{v}(t)$ we apply a noncasual regularized smoothing to the observed output and differentiate numerically. For our model structure we choose e, f polynomial in each x_i (degree 4) and f affine in u. As our observation is a state, we fix our model's $g(x, u)$ to be the membrane potential.

As the response is nearly periodic, we avoid repetitive data by picking approximately 500 data points uniformly spread throughout the $(\tilde{x}, \tilde{v}, \tilde{u})$ space. We minimize $\hat{\mathcal{E}}_Q^0$. For comparison, we also fit a model of the same structure minimizing the equation error, $\sum_i |\epsilon_x(\tilde{z}(t_i))|^2 \rightarrow \min$. In both cases, we insist on an invertible Jacobian $E(x)$ by requiring $E(x) + E(x)' \geq 10^{-3} I$.

Figure 2 plots a neuronal response from the test set and the result of simulating the models from the same initial conditions. Also included is a first order DT model fit using equation error (CT and higher order linear equation error fits led to unstable models).

APPENDIX

A. Live Neuron Experimental Procedure

Primary rat hippocampal cultures were prepared from P1 rat pups, in accordance with the MIT Committee on Animal Care policies for the humane treatment of animals. Dissection and dissociation of rat hippocampi were performed in a similar fashion to [15]. Dissociated neurons were plated at a density of 200K cells/mL on 12 mm round glass coverslips coated with 0.5 mg/mL rat tail collagen I (BD Biosciences) and 4 μg/mL poly-D-lysine (Sigma) in 24-well plates. After 2 days, 20 μM Ara-C (Sigma) was added to prevent further growth of glia.

Cultures were used for patch clamp recording after 14 days in vitro. Patch recording solutions were previously described in [16]. Glass pipette electrode resistance ranged from 2-4 MΩ. Recordings were established by forming a GΩ seal between the tip of the pipette and the neuron membrane. Perforation of the neuron membrane by amphotericin-B (300 μg/mL) typically occurred within 5 minutes, with resulting access resistance in the range of 10-20 MΩ. Recordings with leak currents smaller than -100 pA were selected for analysis. Leak current was measured as the current required to voltage clamp the neuron at -70 mV. Synaptic activity was blocked with the addition of 10 μM CNQX, 100 μM APV, and 10 μM bicuculline to the bath saline. Holding current was applied as necessary to compensate for leak current.

REFERENCES

[1] L. Ljung, *System Identification: Theory for the User*, 3rd ed. Englewood Cliffs, New Jersey, USA: Prentice Hall, 1999.

[2] J. Sjöberg, Q. Zhang, L. Ljung, A. Benveniste, B. Delyon, P.-Y. Glorennec, H. Hjalmarsson, and A. Juditsky, "Nonlinear black-box modeling in system identification: a unified overview," *Automatica*, vol. 31, no. 12, pp. 1691–1724, 1995.

[3] M. Farina and L. Piroddi, "Simulation error minimization identification based on multi-stage prediction," *International Journal of Adaptive Control and Signal Processing*, 2010.

[4] S. L. Lacy and D. S. Bernstein, "Subspace identification with guaranteed stability using constrained optimization," *IEEE Transactions on Automatic Control*, vol. 48, no. 7, pp. 1259–1263, 2003.

[5] A. Megretski, "H-infinity model reduction with guaranteed suboptimality bound," in *Proceedings of the 2006 American Control Conference*, 2006, pp. 448–453.

[6] K. C. Sou, A. Megretski, and L. Daniel, "Convex relaxation approach to the identification of the wiener-hammerstein model," in *47th IEEE Conference on Decision and Control*, Dec 2008.

[7] ——, "A quasi-convex optimization approach to parameterized model order reduction," *IEEE Transactions on Computer-Aided Design of Integrated Circuits and Systems*, vol. 27, no. 3, pp. 456 –469, Mar 2008.

[8] A. Megretski, "Convex optimization in robust identification of nonlinear feedback," in *47th IEEE Conference on Decision and Control*, Cancun, Mexico, Dec 2008, pp. 1370 –1374.

[9] ——, "Systems polynomial optimization tools (spot)," 2010. [Online]. Available: http://web.mit.edu/ameg/www/

[10] M. M. Tobenkin, I. R. Manchester, J. Wang, A. Megretski, and R. Tedrake, "Convex optimization in identification of stable non-linear state space models," 2010. [Online]. Available: arXiv:1009.1670

[11] C. T. Chou, M. Verhaegen, and R. Johansson, "Continuous-time identification of siso systems using laguerre functions," *Signal Processing, IEEE Transactions on*, vol. 47, no. 2, pp. 349 –362, feb 1999.

[12] A. Rahimi and B. Recht, "Unsupervised regression with applications to nonlinear system identification," in *Advances in Neural Information Processing Systems 19*, B. Schölkopf, J. Platt, and T. Hoffman, Eds. Cambridge, MA: MIT Press, 2007, pp. 1113–1120.

[13] H. Ohlsson, J. Roll, and L. Ljung, "Manifold-constrained regressors in system identification," dec. 2008, pp. 1364 –1369.

[14] P. A. Parrilo, "Structured semidefinite programs and semialgebraic geometry methods in robustness and optimization," Ph.D. dissertation, California Institute of Technology, May 18 2000.

[15] D. Hagler and Y. Goda, "Properties of synchronous and asynchronous release during pulse train depression in cultured hippocampal neurons," *J Neurophysiol*, vol. 85, no. 6, pp. 2324–34, Jun 2001.

[16] G. Bi and M. Poo, "Synaptic modifications in cultured hippocampal neurons: dependence on spike timing, synaptic strength, and postsynaptic cell type," *J Neurosci*, vol. 18, no. 24, pp. 10 464–72, Dec 1998.